CONF-790655--3

REACTOR VESSEL AND CORE TWO-PHASE FLOW ULTRASONIC DENSITOMETER

A. E. Arave
EG&G Idaho, Inc.
P.O. Box 1625
Idaho Falls, Idaho 83401

MASTER

ABSTRACT

A local ultrasonic density (LUD) detector has been developed by EG&G Idaho, Inc., at the Idaho National Engineering Laboratory (INEL) for the Loss-of-Fluid Test (LOFT) reactor vessel and core two-phase flow density measurements. The principle of operating the sensor is the change in propagation time of a torsional ultrasonic wave in a metal transmission line as a function of the density of the surrounding media. A theoretical physics model is presented which represents the total propagation time as a function of the sensor modulus of elasticity and polar moment of inertia. Changes in propagation times are related to the polar moment of inertia of the sensor and the density of the surrounding media. The difference between the propagation times in air and water is approximately 3 μs depending on the cross-sectional aspect ratio and length of the sensor. The aspect ratio can vary between 3 and 7 depending on design considerations. The thin side of the sensor is oriented into the flow and varies in width from 0.35 to 1.6 mm depending on the mechanical strength required. Separate effects tests and two-phase flow tests have been conducted to characterize the detector. Tests show the detector can perform in a 343°C pressurized water reactor environment and measure the average density of the media surrounding the sensor.

Design and operating characteristics of the magnetostrictive transducer are discussed: size can be as small as 5 mm diameter x 25.4 mm long; maximum operating temperature is greater than 650°C; and the nuclear radiation resistance is $>10^{18}$ nvt.

Steady state air-water tests were conducted to evaluate the effects of flow on the sensor. For superficial air-water velocities greater than 3 m/s, the flow effects are significant when a 6.35- x 1.50-mm sensor is used. In steam-water transient blowdown tests, correlation with a gamma densitometer reference measurement was excellent except during the mist flow conditions near the end of the blowdown. The overall accuracy was within 100 kg/m^3.

NOMENCLATURE

c_t	=	Ultrasonic torsional wave propagation velocity
c_e	=	Ultrasonic extensional wave propagation velocity
d	=	Length of propagation path
t	=	Total propagation time ($t_o + \Delta t$)
t_o	=	Propagation time at initial conditions
Δt	=	Change in propagation time from initial conditions due to density and temperature
Δt_T	=	Change in propagation time from initial conditions due to temperature
Ka	=	Determined by aspect ratio (width to thickness ratio) of bar
J	=	Inertia of bar and surrounding media
G	=	Modulus of elasticity
ρ_m	=	Density of sensor bar
$\Delta\rho$	=	Change in average density of air-water covering the sensor bar surface from initial conditions
ρe	=	Effective density due to the bar inertia loading at initial conditions
T	=	Temperature of bar
T_o	=	Temperature of initial conditions
K_1, K_2, and K_3	=	Empirically derived constants
d	=	Width of sensor

h	=	Thickness of sensor
Z_t	=	Torsional mechanical impedance
Z_w	=	Extensional mechanical impedance in the wire
r	=	Radius of wire
ℓ	=	Length of sensor

1. INTRODUCTION

The ultrasonic densitometer is a unique detector developed for Loss-of-Fluid Test by EG&G Idaho, Inc., at the Idaho National Engineering Laboratory. The ultrasonic densitometer provides density measurements in steam-water mixtures in the reactor vessel for water reactor research experiments. When stainless steel interfaces at instrument penetrations into pressurized water reactor (PWR) environments and the characteristics of magnetostrictive ultrasonic transducers were recognized to have the best survivability, a development program for the densitometer started ten years ago, with the early instrument development for LOFT[1,2,3]. Later, when core inlet and outlet fluid density measurements were needed in LOFT, Panametrics, Inc., further developed the ultrasonic sensor technique to include core inlet requirements[4]. Application of a torsional ultrasonic wave in the sensor was developed by Panametrics, Inc., and a detector was designed and fabricated by EG&G Idaho, Inc., for installation in LOFT[5,6]. Further development work was then started to improve the performance by making the detector smaller and by minimizing two-phase flow and temperature sensitivity for higher velocity applications.

This paper defines the latest densitometer design parameters and performance technology. Section 2 describes the sensor technique and transducer operating principles and the basic impedance matching concepts. Section 3 discusses the system capabilities. Section 4 provides the sensor characteristics that need design considerations. Section 5 describes applications of the technology. Section 6 describes the analytical model of density sensitivity, and Section 7 presents two-phase flow data for specific sensors.

The ultrasonic densitometer for LOFT uses a "through transmission" technique with a transmit and receive transducer. Densitometers with more recent technology use a "pulse-echo" (reflection) technique with one transducer for transmit and receive modes of generation. Both techniques produce the same performance and have similar design characteristics. This paper will only consider the pulse-echo technique since it provides the greatest application versatility.

In the pulse-echo mode, extensional ultrasonic signals are generated with a magnetostrictive transducer and are converted to torsional waves in the sensor at the point of the transmission line to the sensor attachment. Reflections (echoes) are generated at the mechanical impedance mismatches of transmission line and sensor attachments. The propagation time difference between the echoes generated at each end of the sensor is the signal.

2. PRINCIPLES OF ULTRASONIC DENSITOMETRY

The basic principles of ultrasonic densitometry are explained by: (a) the ultrasonic torsional wave sensing technique, (b) the generation of the extensional ultrasonic signal through use of a magnetostrictive transducer, (c) mechanical impedance matching considerations, and (d) pressure boundary considerations.

2.1 Ultrasonic Torsional Wave Density Sensing Technique

The density sensor mechanism in the densitometer is a torsional ultrasonic wave transmission line. This torsional wave propagation velocity is a function of the sensor polar moment of inertia, modulus of elasticity, and sensor material density. Water surrounding the transmission line increases the inertia forces acting on the sensor and decreases the propagation time. Lynworth[4] has given the following analogy, (see Figure 1). "Visualize the spinning of an oar about its axis, alternately clockwise (cw) and counterclockwise (ccw), by the 'handsducer' method. Now let the oar be immersed gradually in

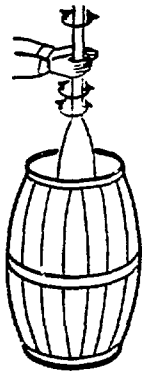

INEL-A-12 275

Fig. 1 Inertia increases proportional to density and depth of immersion.

a nonviscous liquid in a barrel. As the blade enters the liquid, a large increase in inertia is sensed. The more completely the blade is immersed, the more slowly the oar will be spun, for a constant input torque. Once the paddle is fully immersed, deeper immersion makes the circular handle wet, but does not further impede the rotation. The denser the liquid, the greater its inertia, and likewise its resistance to the oar's accelerations."

2.2 Extensional Magnetostrictive Transducer

The generation of an ultrasonic extensional wave in a wire with a magnetostrictive transducer can be explained by considering a wire extending along the x axis with a coil of effective length "b" over a magnetostrictive material of length "b" at the origin, as shown in Figure 2. At zero time, an electric current is induced into the coil. This current magnetizes the length "b" of the magnetostrictive material and produces a packet of strain of amplitude S and length "b" as shown in Figure 3.

This strain travels along the wire with velocity $c = \sqrt{G/\rho_m}$. The pulse has length "b" along the wire and requires time b/c to pass each point of the wire. A step of input current produces an impulse of strain in the Remendur[a] stub; therefore, this strain corresponds qualitatively to the first differential of the current.

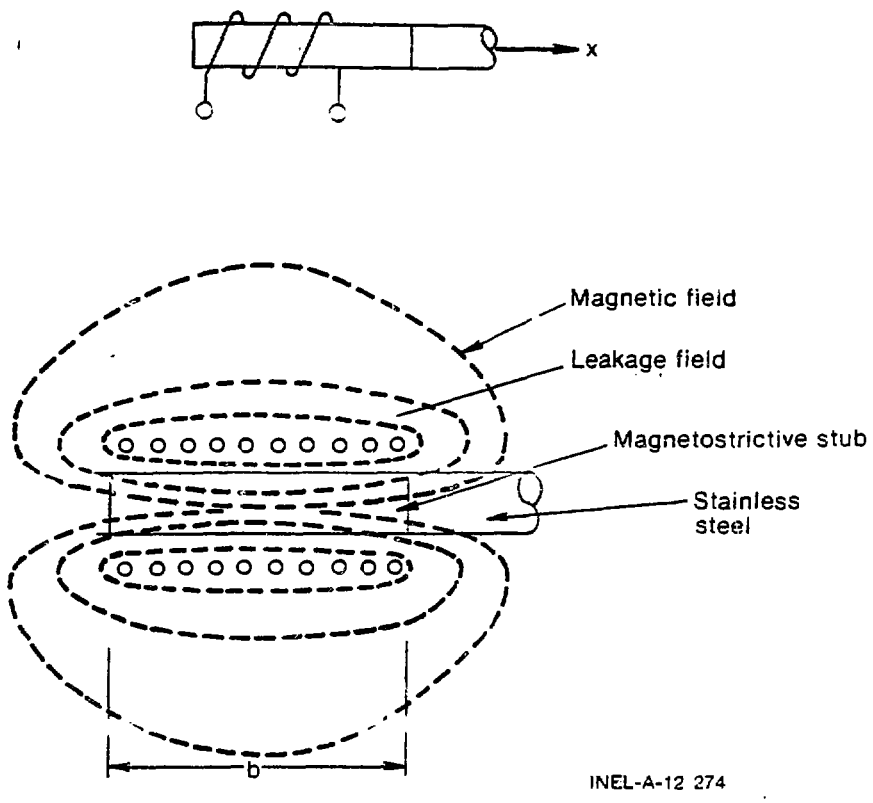

Fig. 2 Transducer electrical diagram.

As the reflected strain pulses from the ends of the sensor enter the transducer, where the magnetostrictive stub of length "b" is located and surrounded by a coil of the same length, the inverse magnetostriction effect generates a magnetic field; the flux linkage with the receiving coil grows uniformly as the strain pulse overlaps more and more of the transducer and falls again as the pulse emerges. This changing magnetic flux "B" induces a receive signal voltage in the coil proportional to $\frac{dB}{dt}$.

When the current is switched back to zero, a similar extensional pulse of the opposite sign is induced so that an unidirectional pulse of current produces in the wire a bidirectional double pulse of strain as shown in Figure 4.

---

a. Remendur is a trade name for a magnetostrictive material made of 49% cobalt, 49% iron, and 2% vanadium.

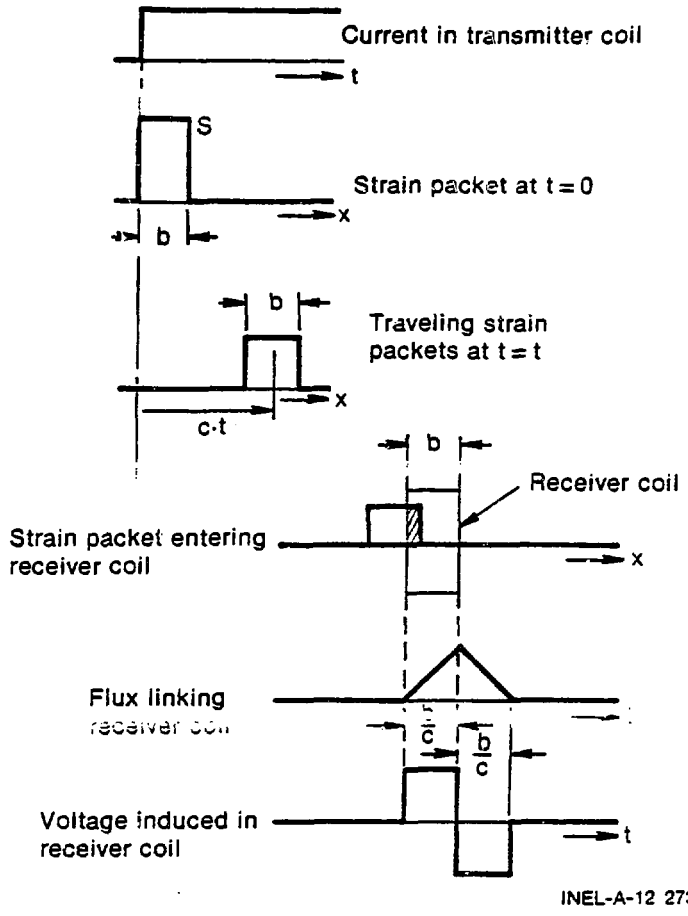

Fig. 3 Idealized waveforms produced by a current step.

In reality, the sharp edges of all the pulses are rounded by the fringe field of the coil, giving waveforms like those shown in Figure 4. As the current pulse is made shorter, the two halves of the mechanical strain pulse move closer together; if the duration of the current pulse is reduced to b/c, the area under the mechanical strain pulse waveform decreases. The optimium waveform is when the two negative cycles of the received signal output voltage overlap each other and result in one negative cycle of twice the original amplitude.

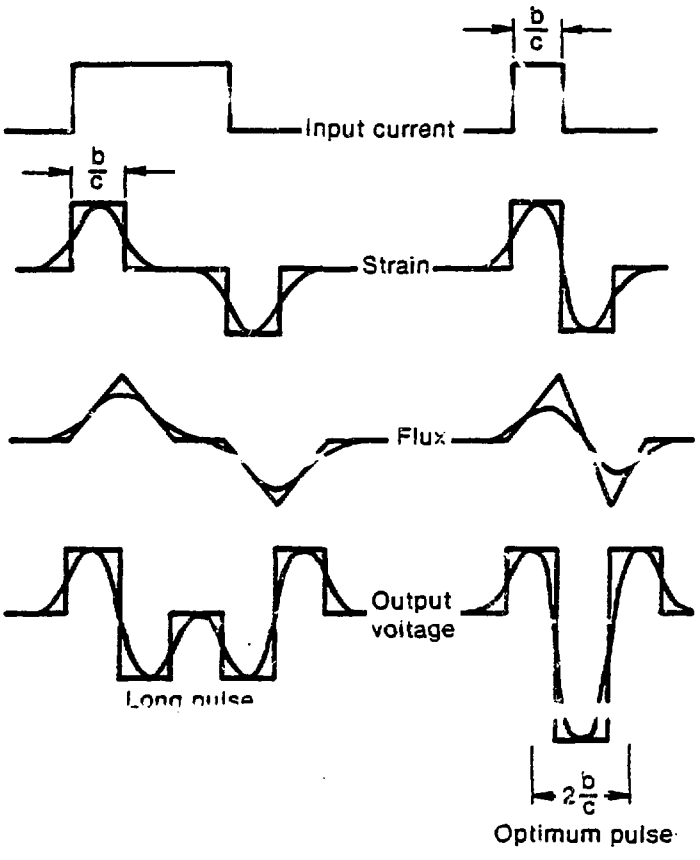

Fig. 4 Wire transmission line wave forms.

2.3 Extensional to Torsional Mechanical Impedance Matching

At the mode conversion from an extensional transmission line wave to a torsional sensor wave, the cross section of the wire should be chosen to give a good mechanical impedance match with the sensor.

The mechanical impedance Z_t for a sensor in torsion is

$$Z_t = \rho_m C_t J \qquad (1)$$

where J is the polar moment of inertia of the cross section of a sensor. For a rectangular sensor

$$J = \frac{dh}{12}(d^2 + h^2) \tag{2}$$

where h is the thickness of the sensor and d is the width.

The torsional impedance presented to the sensor by the transmission line wire is

$$Z_w = d^2 \rho_m C_e A/4 \tag{3}$$

where A is the total cross-section area of the wire.

Matching requires $Z_t = Z_w$ which gives the wire radius as

$$r = \left[\frac{0.33}{\pi} \frac{C_t}{C_e} \frac{h}{d} (d^2 + h^2)\right]^{1/2} \tag{4}$$

Even with wires of optimum size, the impedance match is imperfect and a loss occurs in the mode conversion. The pulse is also lengthened slightly because the wire applies the torque to the sensor over a length essentially equal to the wire width. The pulse in the sensor is lengthened by this amount.

2.4 Penetration Of Welded Pressure Boundaries

Penetration of a welded pressure boundary without destroying the ultrasonic signal is possible using extensional waves. The weld on a transmission line represents a mechanical impedance change that produces an ultrasonic echo. By designing the placement of the welded penetration at a location on the line where an echo is acceptable, interference of unwanted echoes with the signal echoes can be prevented. By making the welded circumferential area around the wire small compared to the cross-sectional area of the wire, the transmitted ultrasonic energy through the boundary is maximized. These requirements are met in the configuration shown in Figure 5. The seal weld of a tube over the wire transmission line is made at the mode

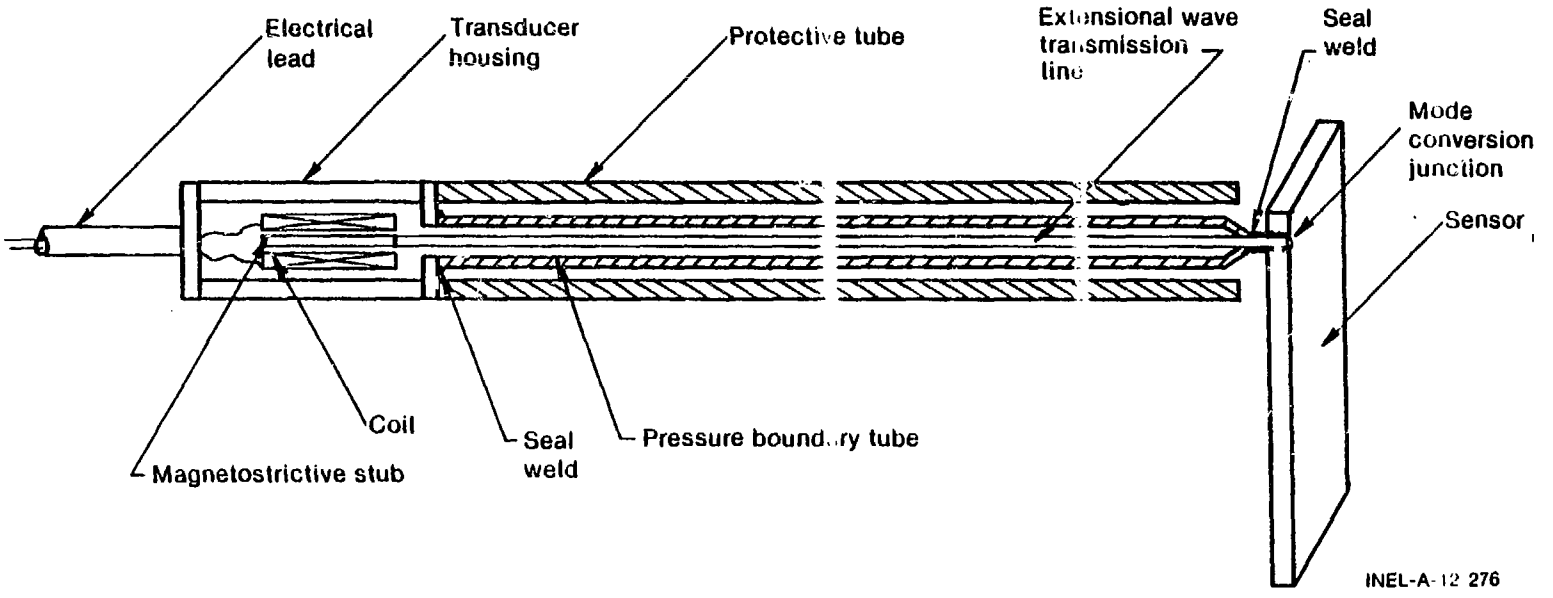

Fig. 5 Pulse-echo pressure boundary configuration.

conversion junction from an extensional to torsional wave. Since part of the ultrasonic energy is transmitted into the tube, the tube is made as long as the extensional wave transmission line to cause the echo from the end of the tube to arrive at the transducer about the same time as the second echo in the transmission wire with the sensor echoes in between (see Section 3 and Figure 6). The other end of the tube is seal welded to the transducer housing. This pressure boundary tube can only be attached at the ends or unwanted echoes will be generated. Mechanical strength and mounting attachment welds must be made to another protective tube placed over the pressure boundary tube attached at the transducer housing.

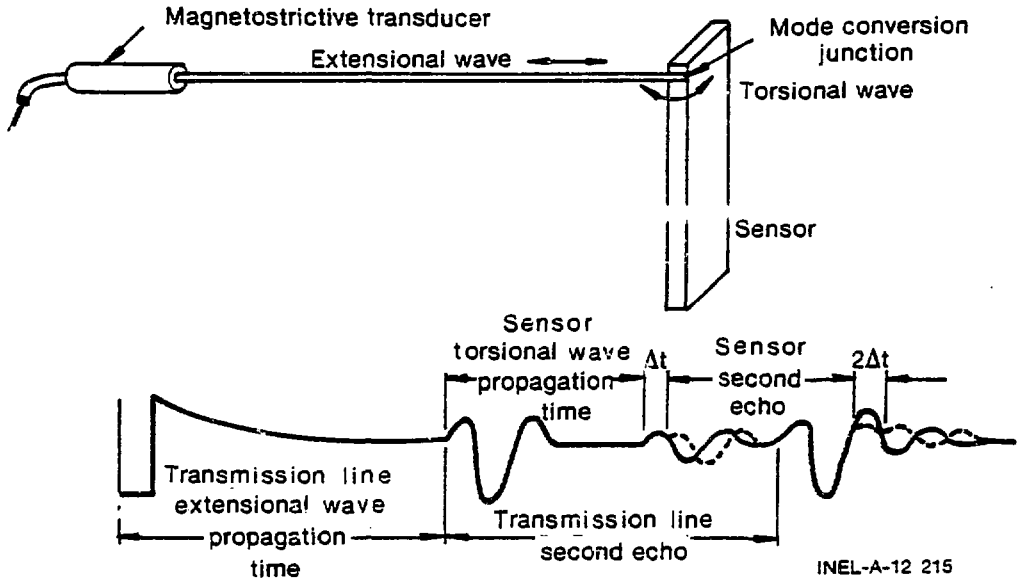

Fig. 6 Basic ultrasonic densitometer detector configuration.

3. ULTRASONIC DENSITOMETER SYSTEM DESCRIPTION

The local ultrasonic densitometer system is described in general in this section. Included are descriptions of the sensor and transducer configuration and the ultrasonic signal and signal processing system. The magnetostrictive transducer generates a 166-kHz extensional stress wave burst that propagates in the extensional wave mode in a wire to the mode conversion junction where it is converted to a

torsional wave in a stainless steel sensor as illustrated in Figure 6. The torsional wave reflects as an echo from the end of the sensor and is received by the same transducer that transmitted it. Echos also arise at each of the changes in transmission line mechanical impedance and have various amplitudes depending on the impedance mismatch.

A block diagram of the pulse echo signal processing system is shown in Figure 7. The basic operating principle is an accurate time interval measurement. The accuracy is controlled by the 0.01-μs electronic time interval resolution for a 1- to 4-μs full scale air-water propagation time change from air to water. The 166-kHz ultrasonic received signal packet is processed through a 100- to 200-kHz band pass filter. Changes in propagation time are measured between the mode conversion extensional wave echo at one end of the sensor and the torsional wave echo from the opposite end of the sensor, as illustrated in Figure 6. Blanking and amplitude discrimination logic are used to allow the zero-crossing detector to provide a pulse for the predetermined zero-crossing reference echos desired. The air-water density sensitivity, the difference in propagation time between air and water, is kept less than a period for ease in tracking the signal within a fixed zero crossing acceptance window. An analog output proportional to the length of the time interval measured is provided.

The magnetostrictive ultrasonic transducer technology is the same as that used for in-pile ultrasonic fuel centerline thermometry[7,8]. Figure 8 shows a typical magnetostrictive ultrasonic transducer. The transducer has demonstrated the capability to withstand temperatures of 900°C with certain ceramic insulation, electrical conductor material, and splicing technique used. All materials are capable of surviving in a nuclear environment, $>10^{18}$ nvt. A typical transducer provides a stress wave burst with a 166-kHz frequency when a 1-mm diameter, 13-mm long Remendur magnetostrictive stub is issued. The coil is also 13 mm long and is contained in a stainless steel housing, 5 mm in diameter and 25 mm long.

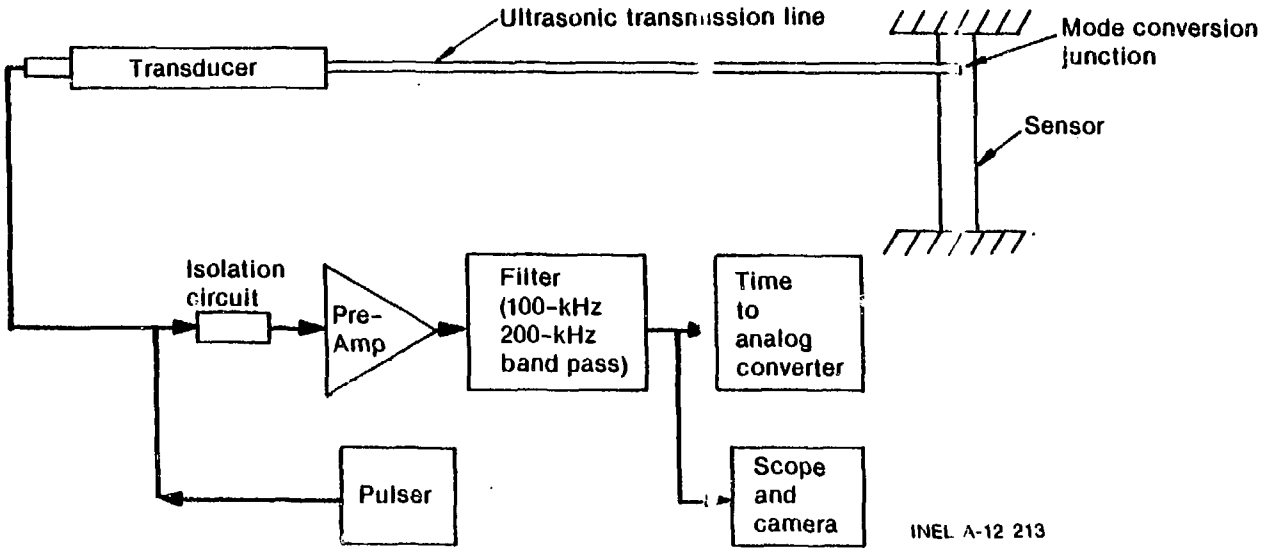

Fig. 7 Ultrasonic densitometer system block diagram.

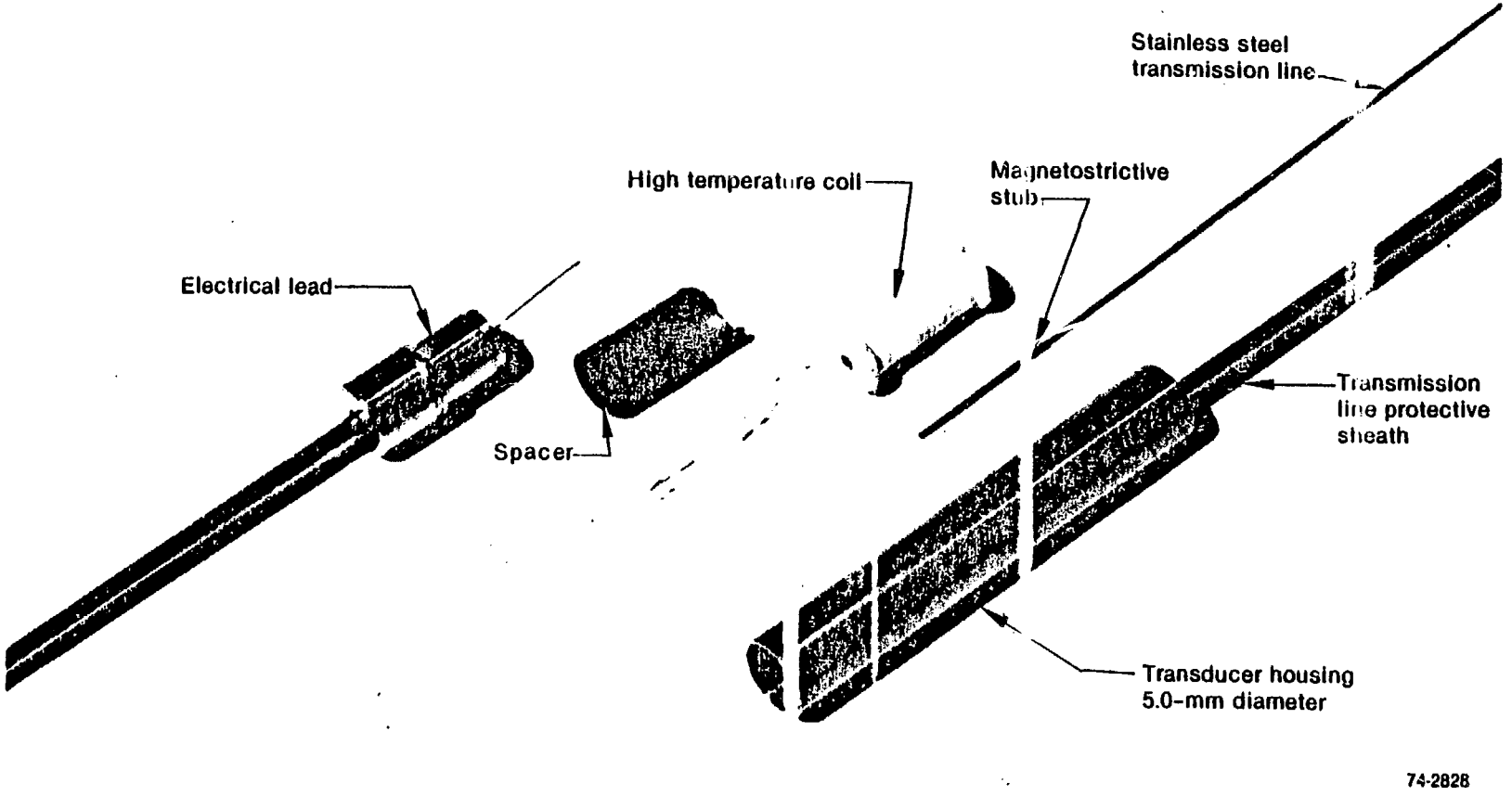

Fig. 8 A typical magnetostrictive, ultrasonic transducer.

4. SENSOR CHARACTERISTICS

The significant sensor characteristics for this paper are sensitivity to density versus size and shape of the sensor, temperature sensitivity, and shape versus separation of the two-phase flow from the sensor surfaces. Other characteristics are pressure sensitivity, wetting response, and ultrasonic signal to noise ratios.

4.1 Density Sensitivity

The sensitivity of the sensor to the density of the single-phase fluids has been shown by Lynworth[4] to be directly proportional to torsional wave propagation time and a function of sensor width to thickness aspect ratio. Typical calibration of propagation time with respect to fluid density is shown in Figure 9. The propagation velocity as a function of aspect ratio for rectangular, wedge, and oval shaped sensor was checked for design purposes and is plotted in Table I. The percentages of air-to-water propagation time changes were also checked and are listed in Table I and plotted in Figure 10. These data indicate that the larger the aspect ratio the longer the propagation time; and for a larger aspect ratio the length must be shortened to have the equivalent propagation time and density sensitivity. Density sensitivity versus aspect ratio is an important design consideration for optimizing size and sensitivity. The percentage change in propagation time versus aspect ratio is plotted in Figure 10 for reference. Other shape considerations noted were:

(1) Large aspect ratios generate a dispersive wave that deteriorates in shape with distance but usually is not a problem since the sensors are too short to see this effect.

(2) Shapes other than rectangular do not have as distinctive a torsional wave envelope and are dispersive, but in many cases do provide a density sensitivity and signal envelope shape that is useful.

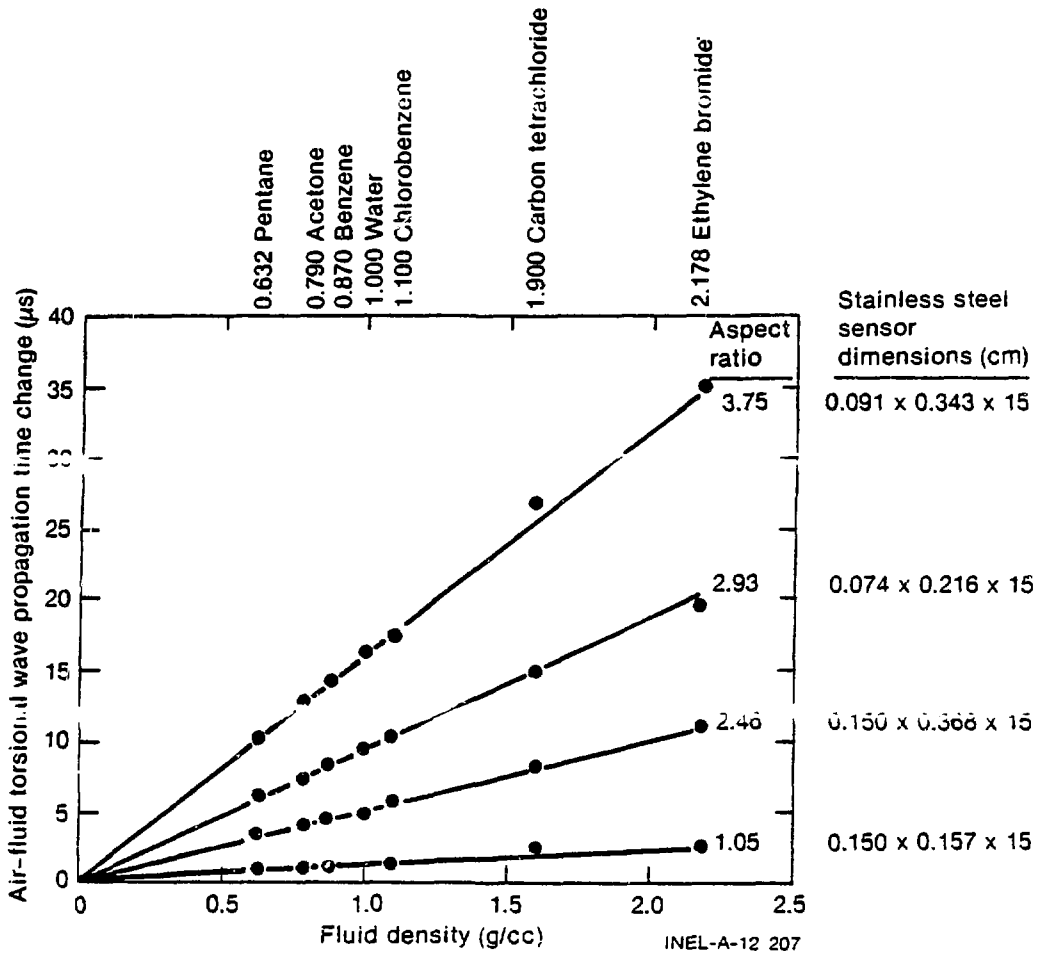

Fig. 9 Single-phase density calibration data.

4.2 Temperature Sensitivity

The ultrasonic propagation time in the sensor is a well defined function of the modulus of elasticity and density of the sensor material. The propagation time modulus of elasticity temperature sensitivity can be a problem to compensate for under transient temperature conditions but can be reduced by selection of a material that has a small change in the modulus of elasticity versus temperature.

The propagation time in a transmission line with density constant is given by

TABLE I

ULTRASONIC DENSITY SENSOR SHAPE VERSUS PERFORMANCE CHARACTERISTICS

Shape	Size (mm)	Aspect Ratio (width/ thickness)	Air-Water Propagation Time (to μs/cm)	Density (% t_o)
Oval	2.28 x 6.35 x 34.92	4.16(avg)	8.6	5.8
Air foil	1.52 x 6.35 x 34.92	8.32(avg)	11.4	13.7
Air foil	0.99 x 3.30 x 17.78	6.50(avg)	12.6	11.1
Rectangular	1.52 x 6.35 x 34.92	4.16	8.6	7.0
Rectangular	0.99 x 6.35 x 34.92	6.25	9.7	9.0
Rectangular	0.99 x 3.30 x 34.92	3.25	10.3	5.5
Rectangular	0.56 x 3.17 x 18.79	5.68	12.8	8.3
Rectangular	0.35 x 2.44 x 17.78	7.14	13.2	13.2

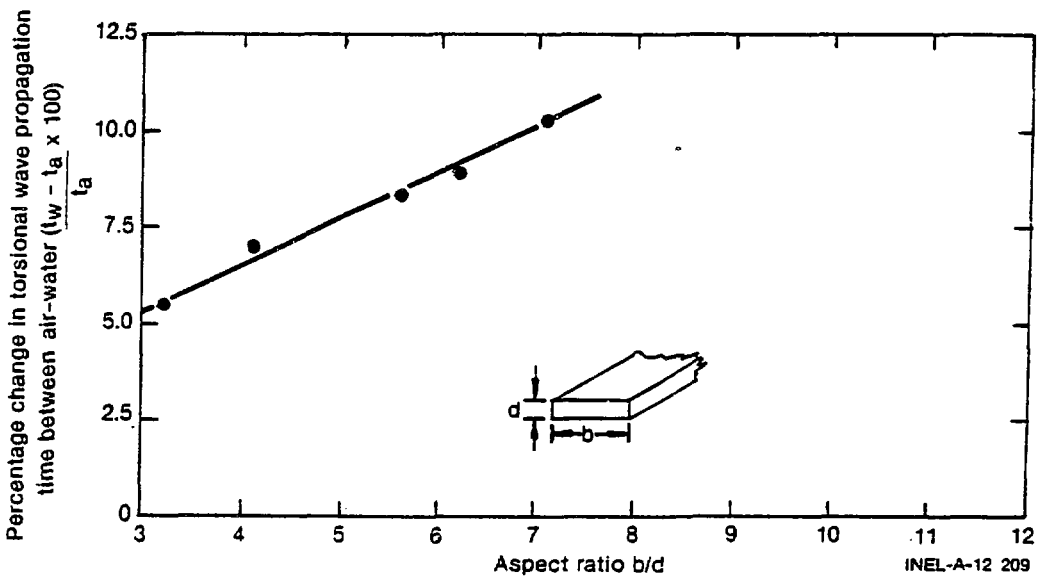

Fig. 10 Air-water density sensitivity versus sensor aspect ratio.

$$t = \frac{d}{c} = d\sqrt{\rho m/G} \cdot \qquad (5)$$

The differential delay is therefore given by

$$\frac{dt}{t} = \frac{dd}{d} + \left(\frac{1}{2} \times \frac{d\rho}{\rho}\right) + \left(\frac{1}{2} \times \frac{dG}{G}\right) \qquad (6)$$

but

$$\frac{d\rho}{\rho} = -3\,\frac{dd}{d}$$

so

$$\frac{dt}{t} = -\frac{1}{2}\left(\frac{dd}{d} - \frac{dG}{G}\right).$$

The zero temperature coefficient of delay, therefore, requires the temperature coefficients of linear expansion and of elasticity to be equal and of opposite polarity. This requirement is the basis for some modern alloys which have been developed.

In binary nickel-iron alloys, the temperature coefficient of elasticity is zero at about 27% and 44% nickel and varies rapidly with composition near these values. At 45% nickel, the coefficient is negative by just enough to balance the coefficient of expansion.

The addition of titanium gives a precipitation-hardening alloy in which the effective nickel content can be controlled by critical heat treatment during which nickel is precipitated as a nickel-titanium compound. The further addition of chromium makes the heat treatment less critical. Alloys developed in this way are known as Ni-Span C.

Such materials are Incoloy 902 (Elinvar) and Incoloy 903 (Ni-Span C) with the chemical composition shown in Table II. Temperature sensitivity tests in the oven up to 350°C show the improvement over stainless steel to be a factor of ten, as shown in Figure 11.

The exact characteristic of all metallic materials depends on the exact composition, the degree of cold working, and the heat treatment.

TABLE II

ELINVAR AND INCOLOY 903 CHEMICAL COMPOSITION

Elements	Incoloy 902 [Elinvar (%)]	Incoloy 903 (%)
Nickel	45	38
Chromium	5	--
Titanium	2.75	1.4
Carbon	0.04	--
Aluminum	0.30	0.40
Silicon	0.50	--
Cobalt	0.35	15
Columbium	--	3
Iron	Balance	Balance

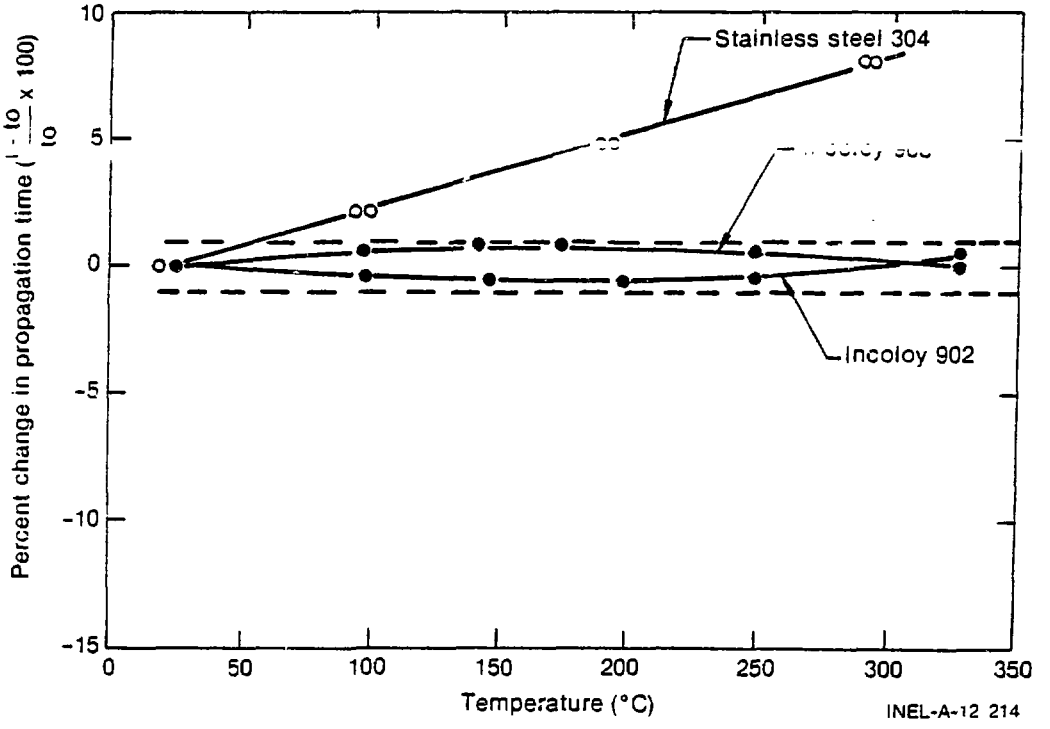

Fig. 11 Percentage change in propagation time versus temperature.

4.3 Sensor Shape

The hydrodynamic shape of the sensor in two-phase flow greatly affects the accuracy at higher velocities. The deflected inertia of

the flow at the front edge of the sensor can cause separation of the flow from the sensor surface. In the resultant recirculation zone, air in bubbly flow and water in mist flow are captured. A worse case illustration is shown in Figure 12. Under these conditions, as shown in the two-phase flow performance data presented subsequently, the measured density is not indicative of the density of the impingent two-phase flow on the sensor. Data were taken in worse case bubble flow and mist flow conditions with various sensor shapes to characterize the errors. The bubbly flow data are shown in Figures 13, 14, and 15. The wedge-shaped hydrofoil provides the best results with the angle of flow attack parallel to the sensor thin axis as shown in the shape comparison data in Figure 13. With the sensor oriented perpendicular to the flow, the recirculation zone is limited to the backside of the sensor. For sensors with flow separation on both sides in parallel flow, perpendicular flow cuts the errors in half as can be seen by comparing Figures 13 and 14. Errors can be reduced further by designing a sensor with the back side not sensitive to the flow. For ambient conditions, this design was accomplished by coating one side of the sensor with RTV[a]. The results are shown in Figure 14. With the density sensitive surface perpendicular to the flow, the criticality of the angle of attack that causes separation of the flow is reduced from a few degrees to almost 90 degrees as shown in Figure 16.

In conclusion, the wedge-shaped sensors have been shown to be viable for use as transmission lines for torsional waves over short distances and are density sensitive. With this verification in bubbly and mist flows, a classical fluid dynamics theory can be used to design sensors for optimum gas and/or water velocities depending on the measurement requirements.

---

a. Room temperature vulcanizing (RTV) is a trade name for a silicone rubber sealant made by General Electric or Dow Corning.

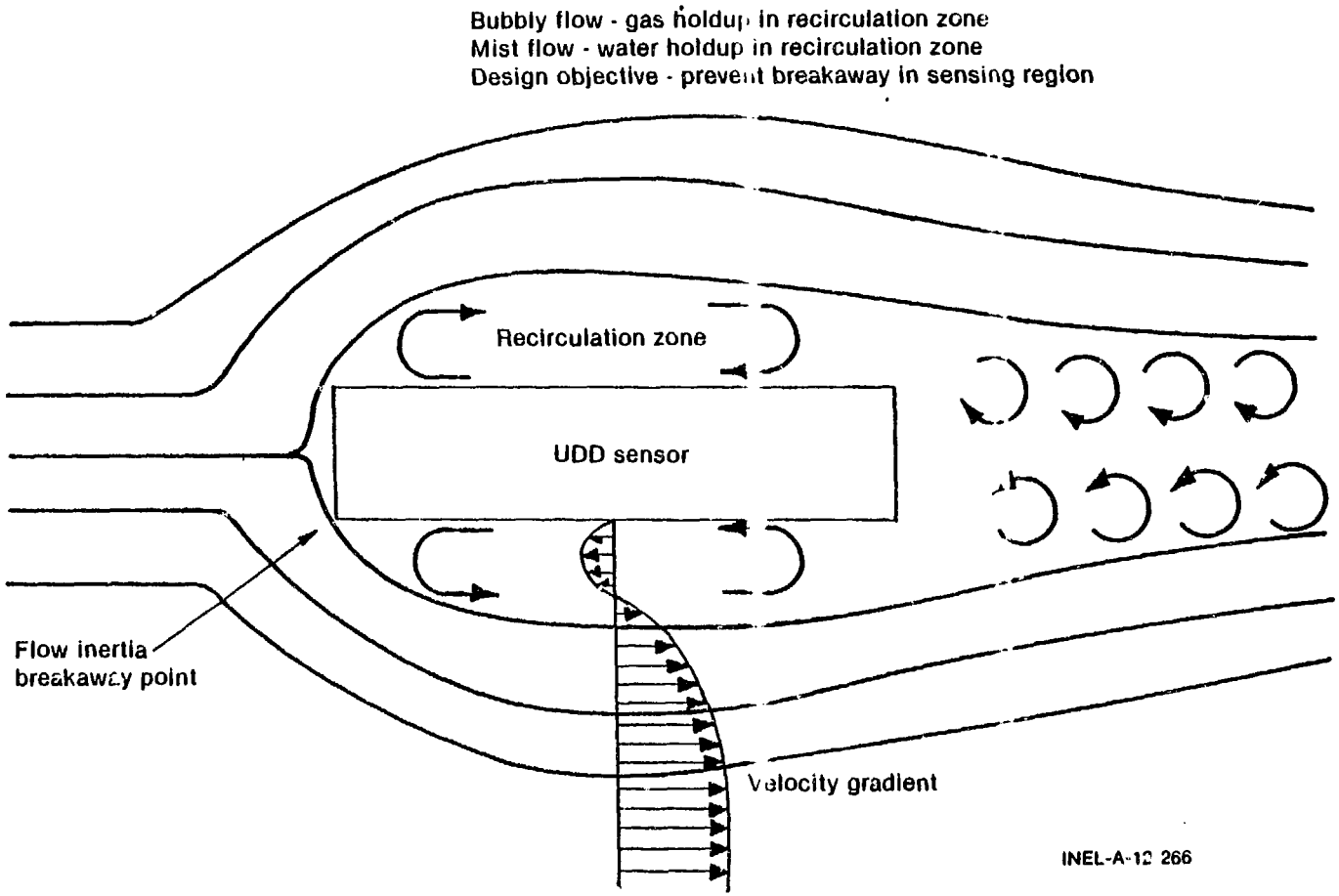

Fig. 12 High velocity flow separation.

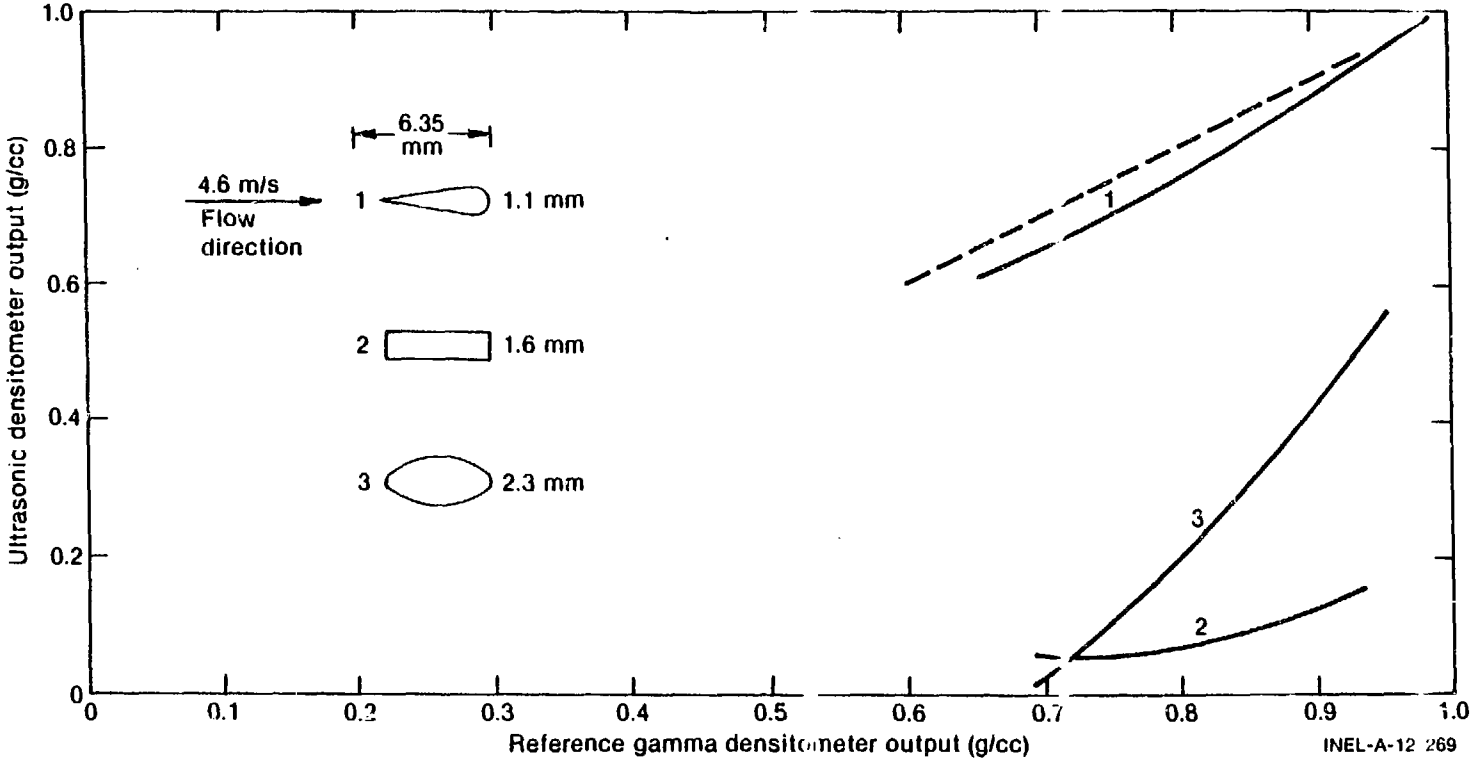

Fig. 13 Sensor shape versus bubble flow performance.

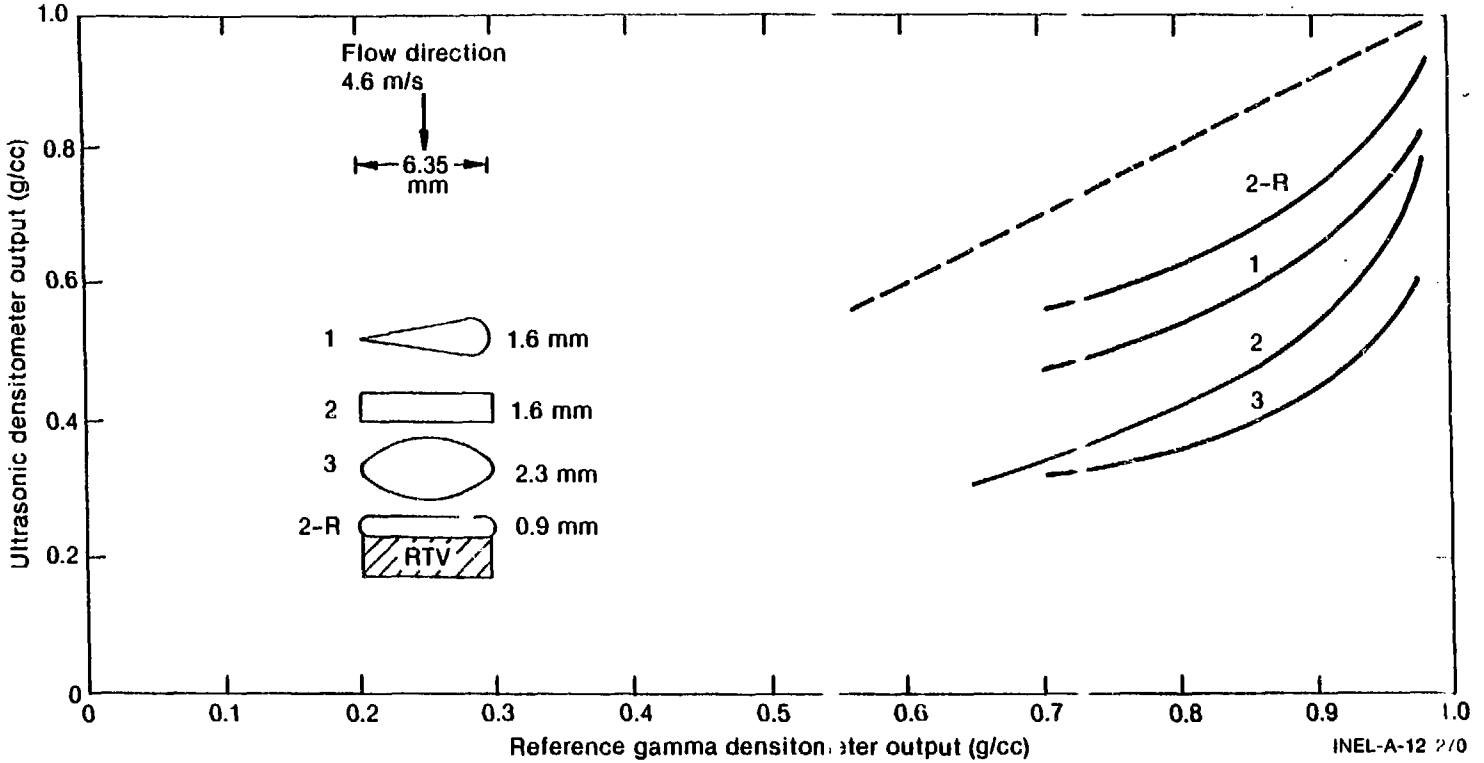

Fig. 14 Perpendicular flow characteristics.

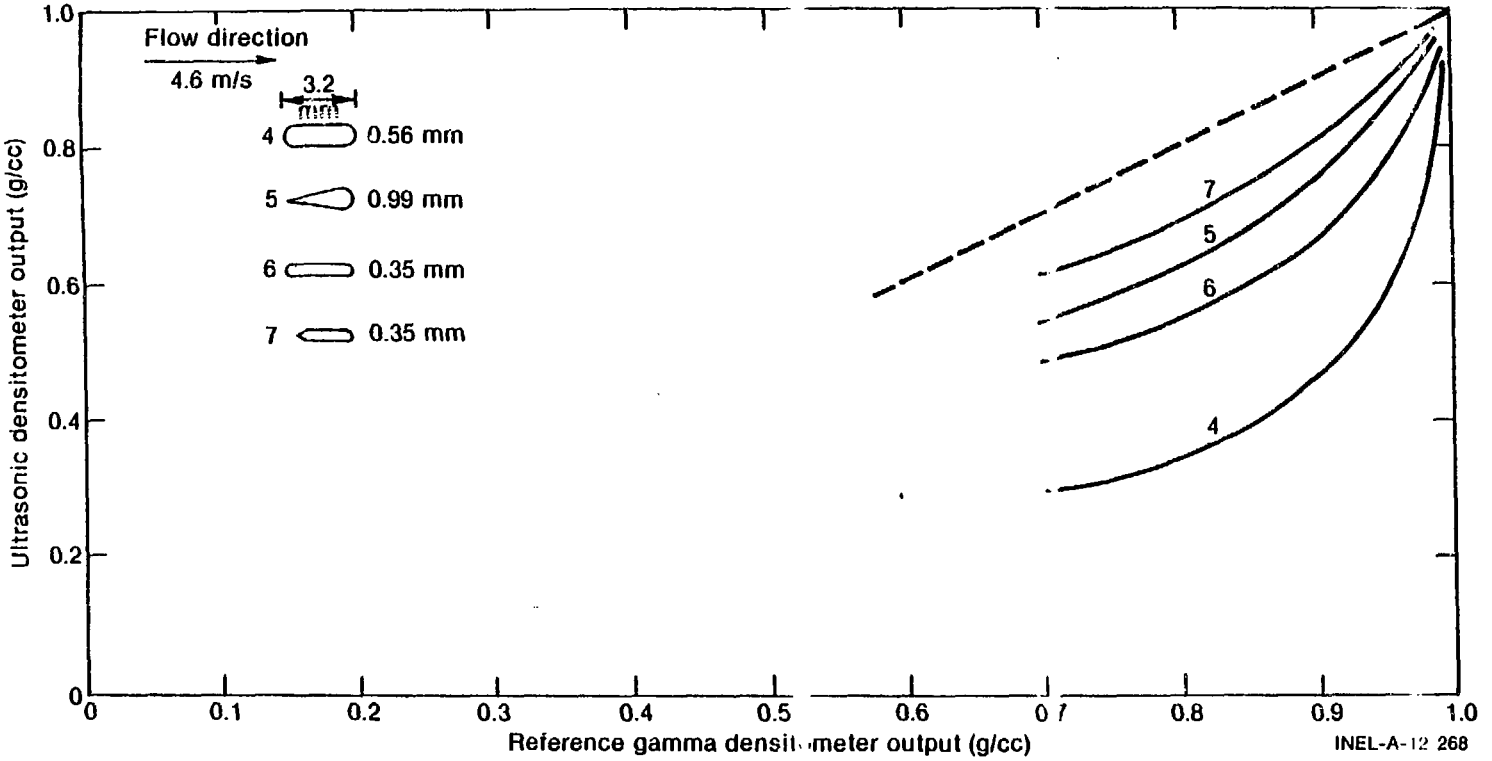

Fig. 15 Small sensor shape versus bubbly flow performance.

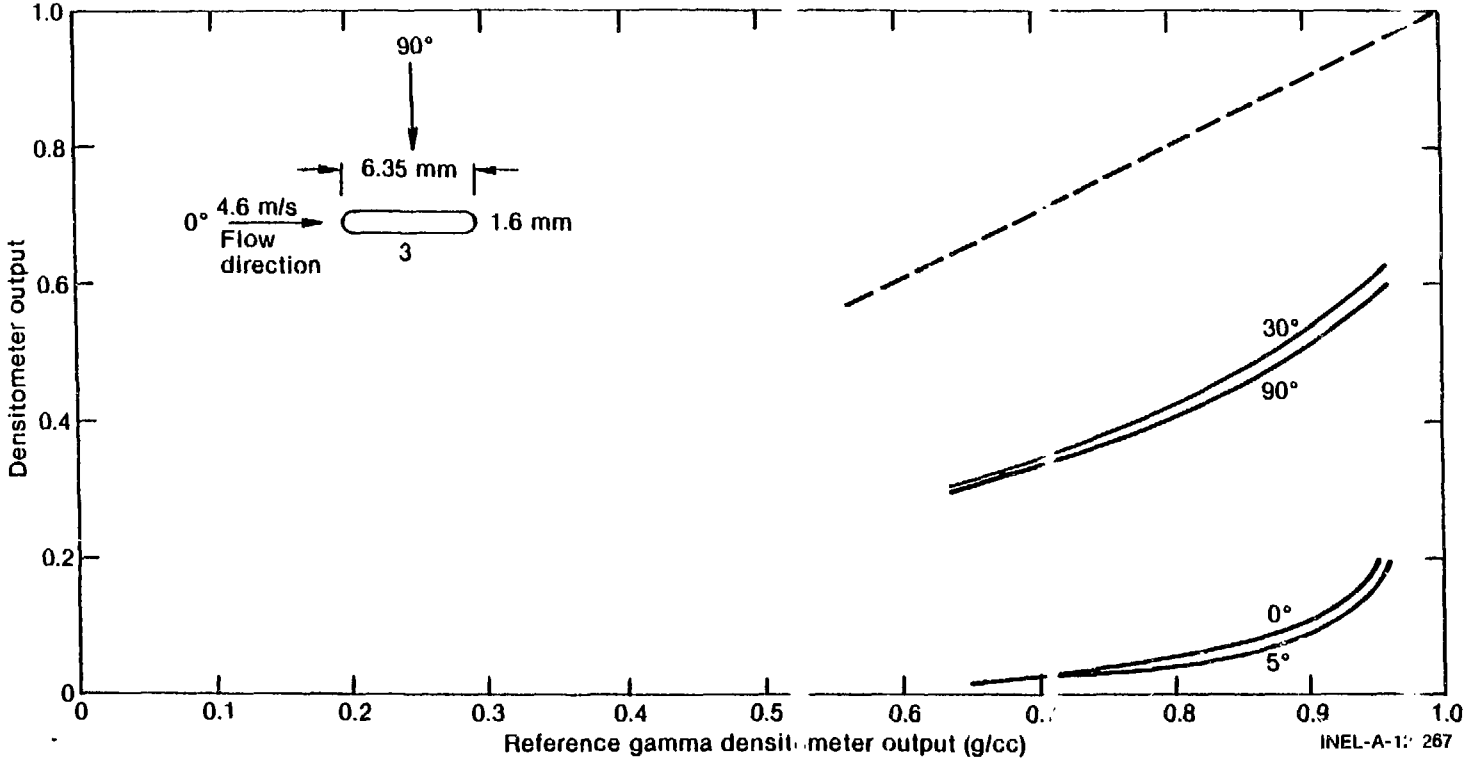

Fig. 16 Bubble flow performance versus angle of attack.

4.4 Other Characteristics

Pressure sensitivity does not exist for the ultrasonic densitometer except when the density at the sensor surface has pressure dependence; such as, gas bubbles collected on the sensor surface under static flow conditions. Sensitivity has been checked at pressures up to 34.5 MPa.

The wetability of the sensor surface does not affect performance under static flow conditions. Under bubbly flow conditions a smoother surface delays flow separation until higher superficial water velocities are reached.

The wetting response when inserting the sensor into water is controlled by the size of the splash and water inertia response time to collapse back on the sensor surface. A typical response is about 25 ms.

Maximum errors possible when the signal phase is shifted by ultrasonic noise mixing with the signal has been calculated and verified with empirical data. The phase shift versus noise ratio function is shown in Figure 17. For a 100-kHz signal with a signal to noise ratio of five, the maximum phase shift possible is 0.3 μs. For an air-to-water density sensitivity of 3 μs, the output variation would be as high as 10%.

5. POSSIBLE ULTRASONIC DENSITOMETER CONFIGURATIONS

Many configurations can be designed to meet experiment needs, regardless of spatial restraints and measurement requirements.

The ultrasonic signal can be received by through transmission or pulse-echo transmission with the same sensor performance in each situation. The sensor shape, length, and aspect ratios can be varied over a wide range and still propagate a torsional wave sensitive to

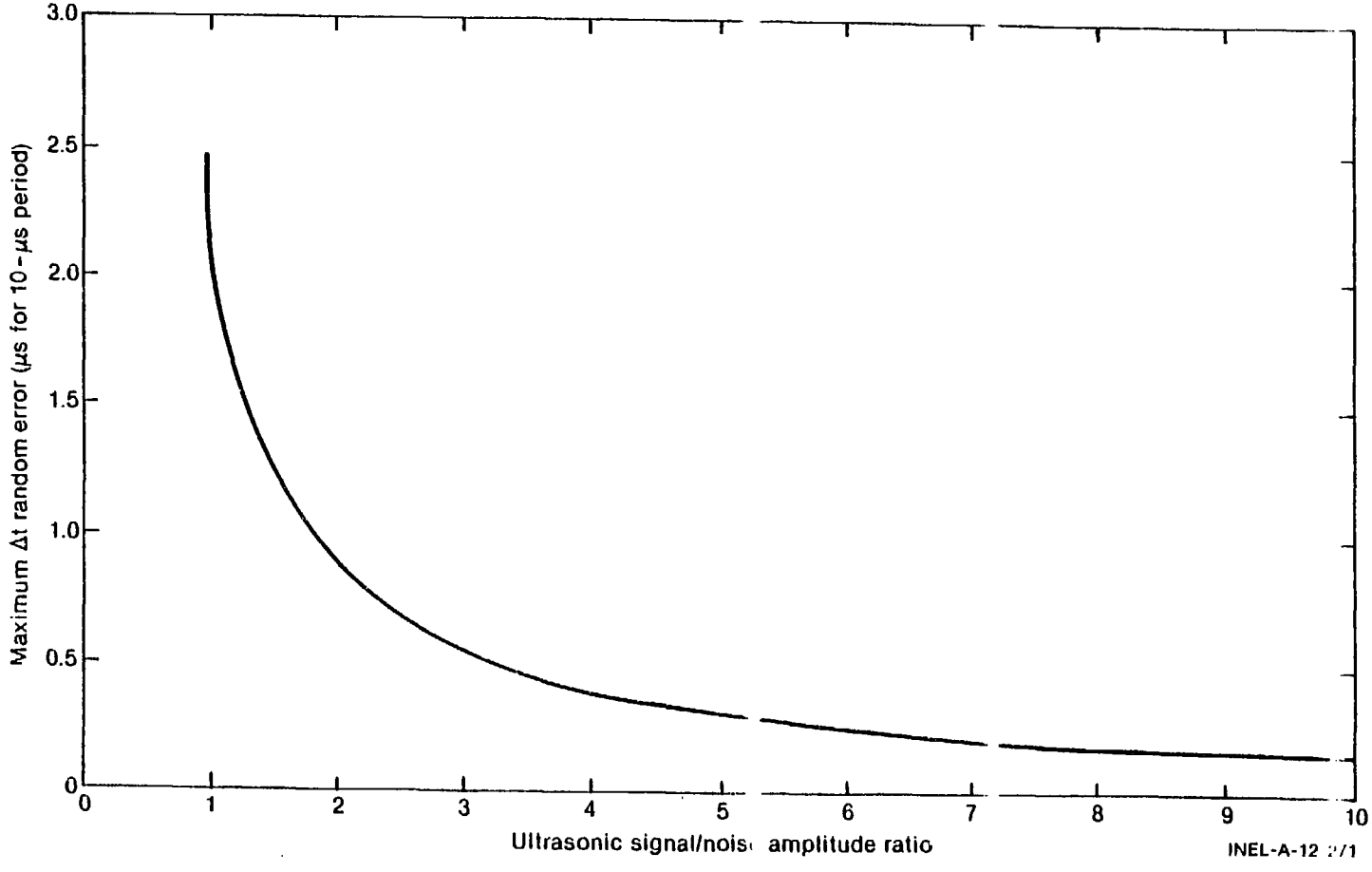

Fig. 17 Propagation time errors versus ultrasonic signal to noise amplitude ratio.

changes in density. For instance, the LOFT core inlet through transmission detector shown in Figure 18 is 6.3 mm wide and 76 mm long and is mounted as shown in Figure 19. A pulse-echo detector constructed for air-water plenum tests has a sensor 2.5 mm wide and 15 mm long as shown in Figure 20, and can be compared with the basic configuration shown in Figure 7.

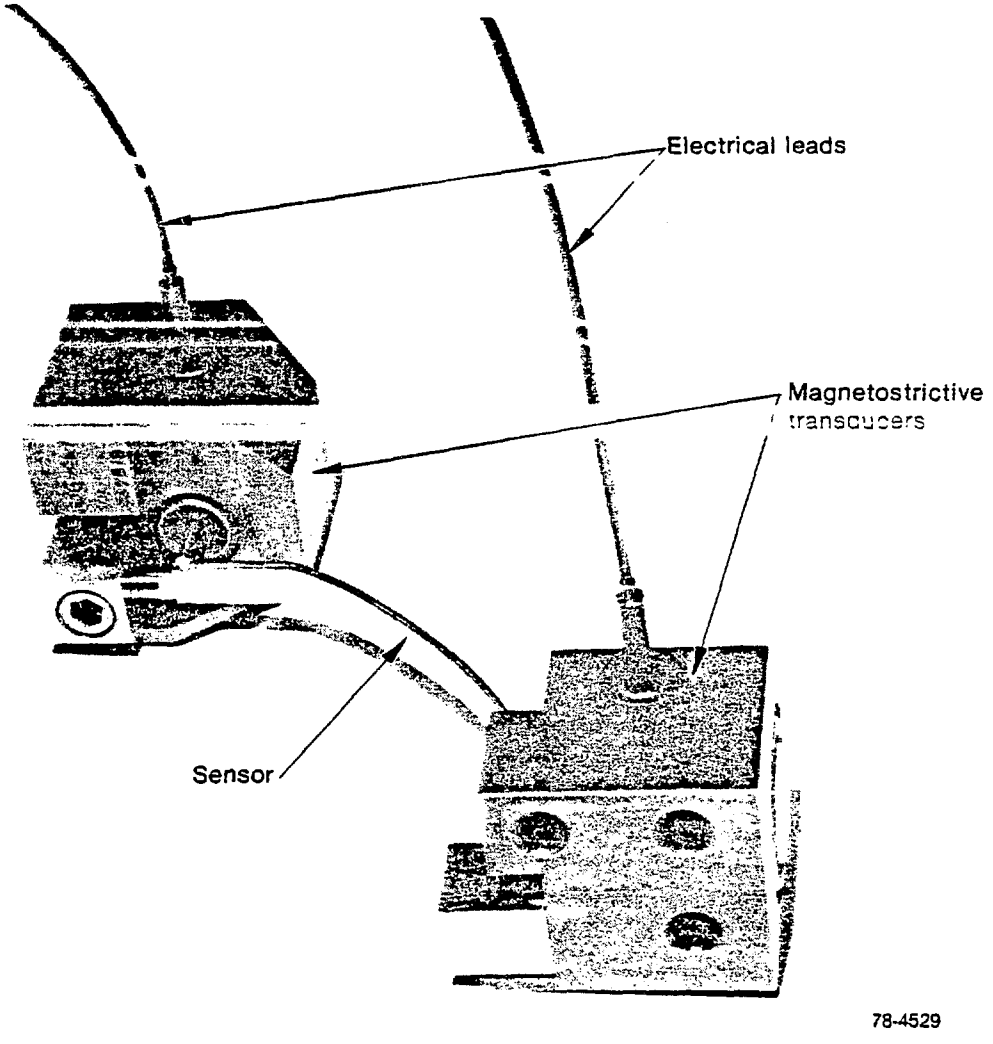

Fig. 18 LOFT core inlet ultrasonic densitometer.

The length of the extensional wave transmission line has a large variable length capability making it possible to extend the length to reach a sensor attached to the spacer grid among a bundle of fuel rods. This possibility has not yet been reduced to application.

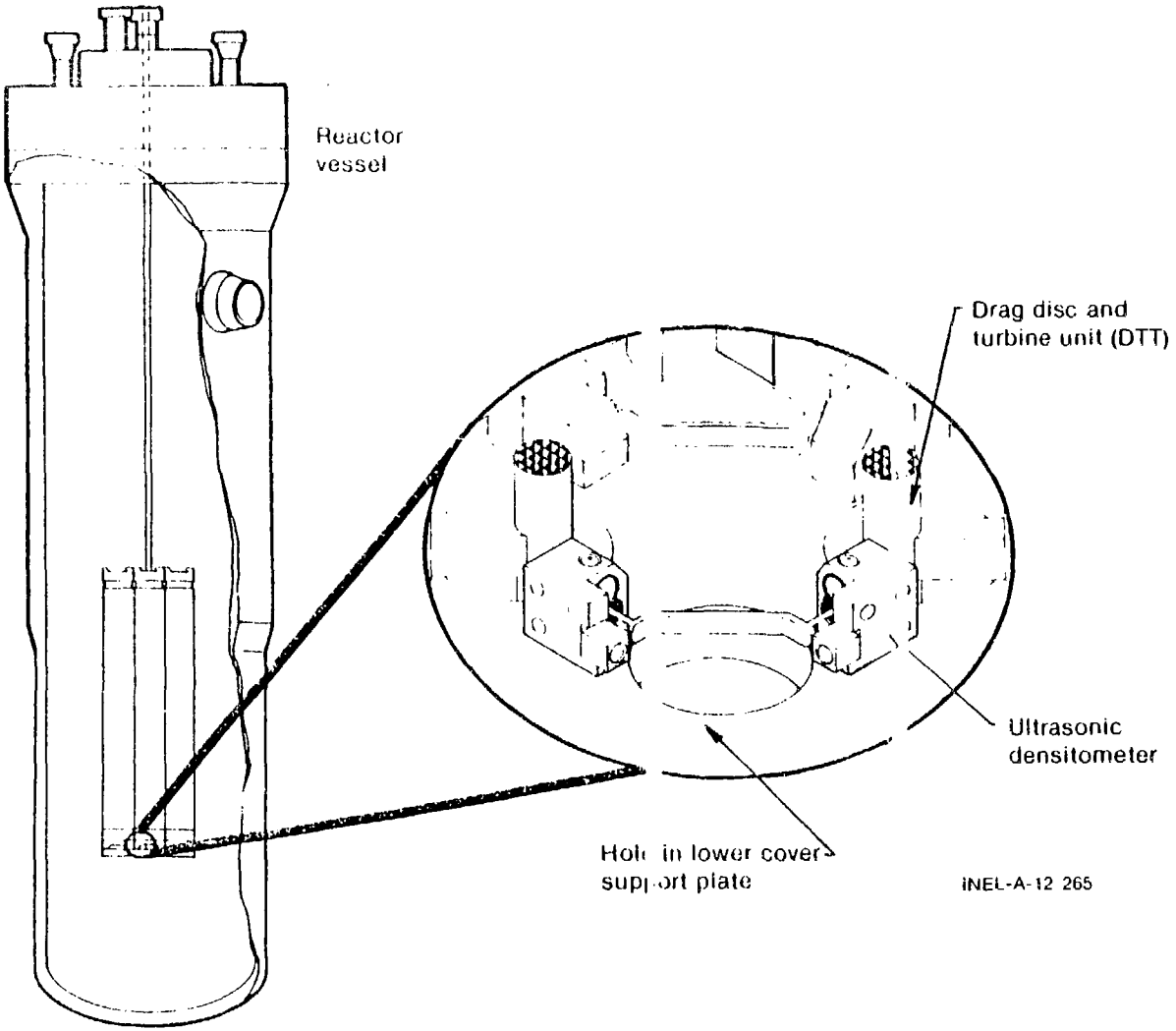

Fig. 19 LOFT core inlet ultrasonic densitometer location.

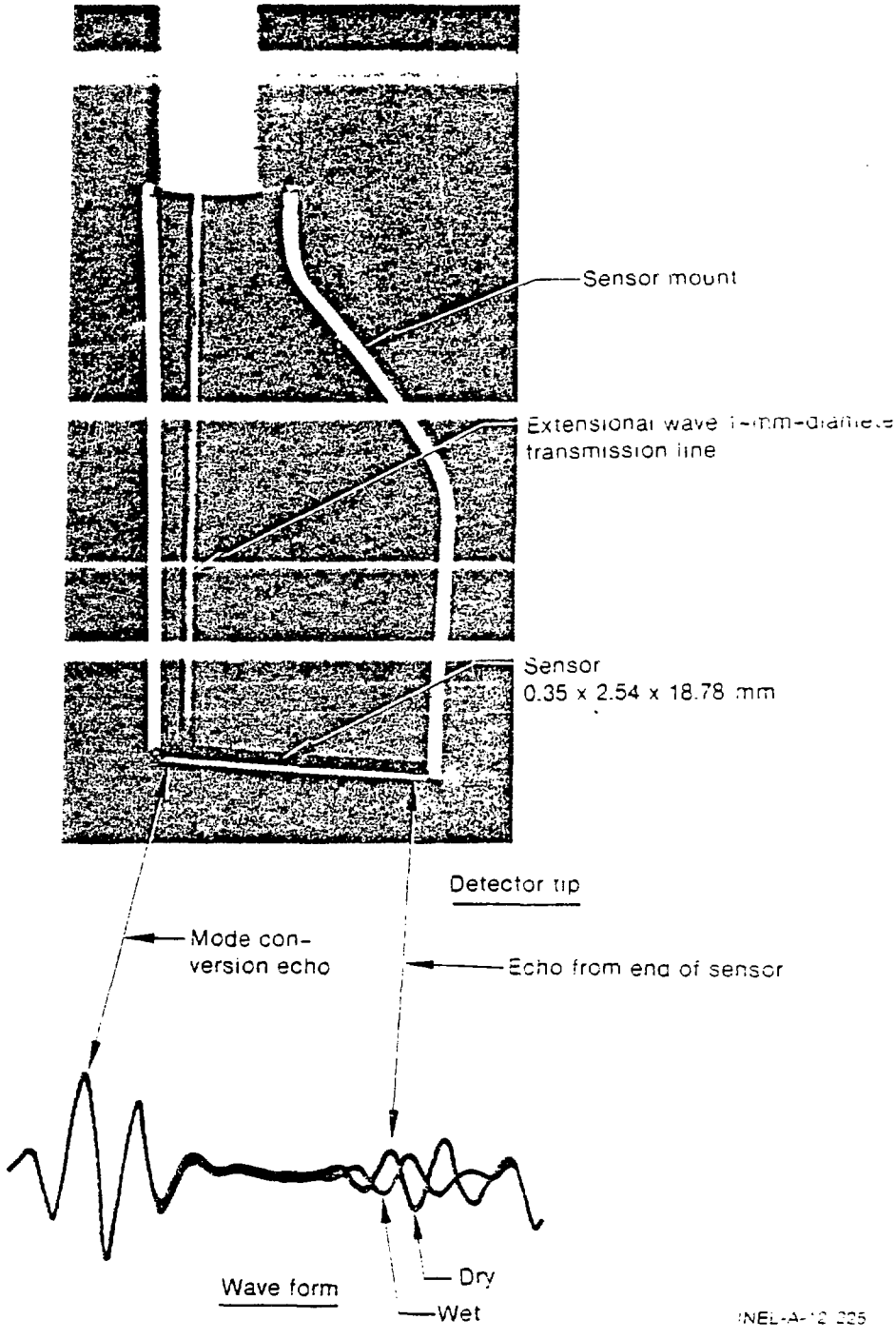

Fig. 20 Air-water plenum test ultrasonic densitometer.

$$\frac{1}{t} = \frac{K_1}{\Delta\rho + \rho e} \quad (K_2 - T)^{1/2} \tag{8}$$

or in terms of the density of the two-phase mixture, the mathematical model is

$$\Delta\rho = K_1 \; t \; (K_2 - T)^{1/2} - \rho e. \tag{9}$$

In terms of dry initial conditions propagation time and temperature, the dry sensor virtual density where $\Delta\rho = 0$ can be defined as

$$\rho_e = K_1 \; t_o \; (K_2 - T_o)^{1/2}. \tag{10}$$

Substituting Equation (10) into Equation (9) the density of the media surrounding the sensor can be written as

$$\Delta\rho = \left[K_1 \quad (K_2 - T)^{1/2} \; t - (K_2 - T_o)^{1/2} \; t_o\right]. \tag{11}$$

For the oven environment where $\Delta\rho = o$, the normalized propagation time dependence on temperature can be expressed as

$$\frac{t}{t_o} = \frac{t_o + \Delta t_T}{t_o} = \frac{(K_2 - T_o)^{1/2}}{(K_2 - T)^{1/2}} \; . \tag{12}$$

By substituting Equation (12) into Equation (11), the density can be expressed in terms of the measured changes in propagation time

$$\Delta\rho = \frac{K_3 t_o}{t_o + \Delta t_T} \; (\Delta t - \Delta t_T) \tag{13}$$

where Δt_T is the change in propagation time from initial conditions K_2 taken from dry oven test at the same temperature, T, as the sensor temperature when the density is being calculated. The change in propagation time due to temperature (Δt_T) is subtracted from the combined change in density and temperature propagation, Δt, time from

The sensor shape can be made hydrodynamic for large superficial gas and water velocities to reduce errors caused by flow effects. Some possible configurations are shown in Table I with density sensitivity listed.

Multiple echoes from multiple sensors on the same transmission line can be constructed to provide density profile information from one detector. This has been done successfully in the ultrasonic thermometry field (reference). The transducer development has not been performed to reduce this principle to practice for ultrasonic densitometry.

6. ANALYTICAL MODEL OF DENSITY SENSITIVITY

The analytical model determined for density sensitivity relates propagation time to media density at the sensor surface and to sensor bar temperature. From this model, equations are obtained for calculating density in terms of total propagation time, changes in propagation times, sensor temperature, and predetermined constants.

The torsion wave propagation velocity can be expressed as

$$c = \frac{d}{t} = \frac{Ka}{J}\left[\frac{G}{\rho_m}\right]^{1/2}. \qquad (7)$$

To express this equation in terms of changes in propagation time, density and temperature, the modulus of elasticity, G, and the moment of inertia, J, are expressed as functional dependence $G \sim K_2 - T$ and $J \sim \Delta\rho + \rho e$, respectively, where T is the sensor bar temperature, $\Delta\rho$ is the change in the density of the media surrounding the sensor bar, and ρe is the virtual density of the sensor under dry conditions. The length of the propagation path, d, the aspect ratio of the bar, Ka, and the density of the sensor bar, ρ_m, are essentially constant for the material densities and temperatures of concern and are included in one empirical constant, K_1. With this information Equation (7) can be written as

initial conditions. Equation (13) is the equation that provides the density measurement in terms of initial conditions, total propagation time, changes in propagation time, and sensor temperature. A simple analysis of this equation is to note density propagation time changes are the difference of temperature changes initial conditions and wet density and temperature changes and wet density and temperature changes taken from initial conditions, $(\Delta t - \Delta t_T)$; as temperature changes the constant of the same as changing proportionality, $\left(\frac{K_1 t_o}{t_o + \Delta t_T}\right)$, between time and density the sensitivity changes effectively the same as changing the sensor length. The above derivation is for pure torsional waves and may not agree with empirical data from sensors with another mode of propagation mixed in with the torsional mode.

7. TWO-PHASE FLOW MEASUREMENT PERFORMANCE

Performance of the ultrasonic density detector in two-phase flow is as expected for an intrusive two-phase flow density measurement. The average density measured is the sum of the gas and water densities at the sensor surface, but this average density can be different than the average density of the flow impingment on the front surface of the detector. This section illustrates the performance of a rectangular sensor in air-water steady state flow and an oval shaped sensor under transient steam-water conditions. The flow effects discussed in Section 4 under sensor shape are readily apparent in the data.

The performance of the sensor in an air-water environment was tested in four flow regimes with a 6.40- x 0.56-mm rectangular sensor. The ultrasonic densitometer output was compared with that from a gamma densitometer output over approximately the same vertical path. The data for each flow regime are shown in Figures 21, 22, 23, and 24. By visual observation through a transparent test section, two basic flow effects were identified: (a) bubble masking on the sensor surface in the flow separation recirculation zones and (b) mist flow droplet holdup in the recirculation zone on the sensor surface.

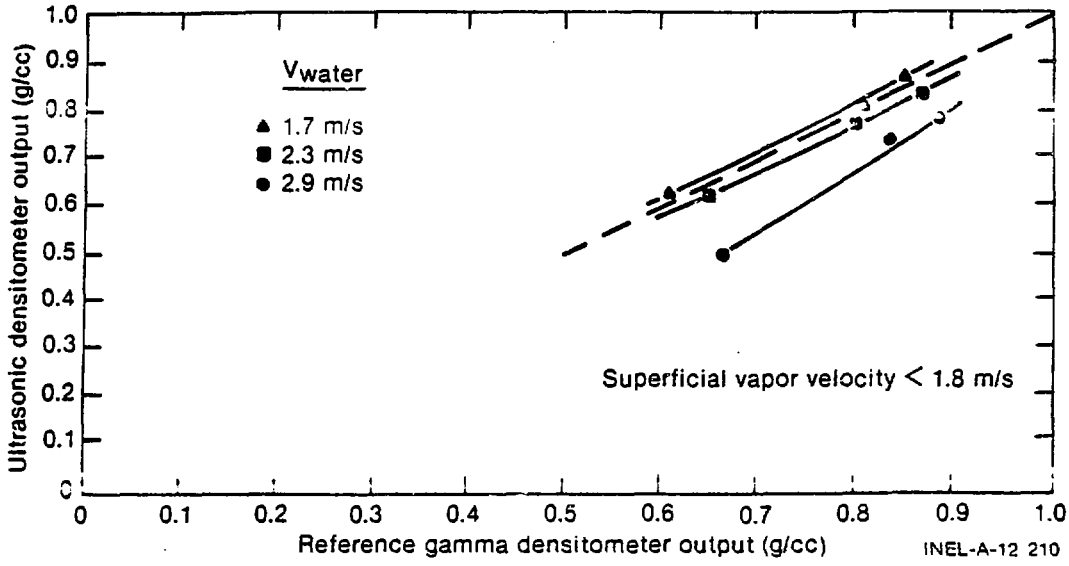

Fig. 21 Ultrasonic versus gamma densitometer stratified and slug flow.

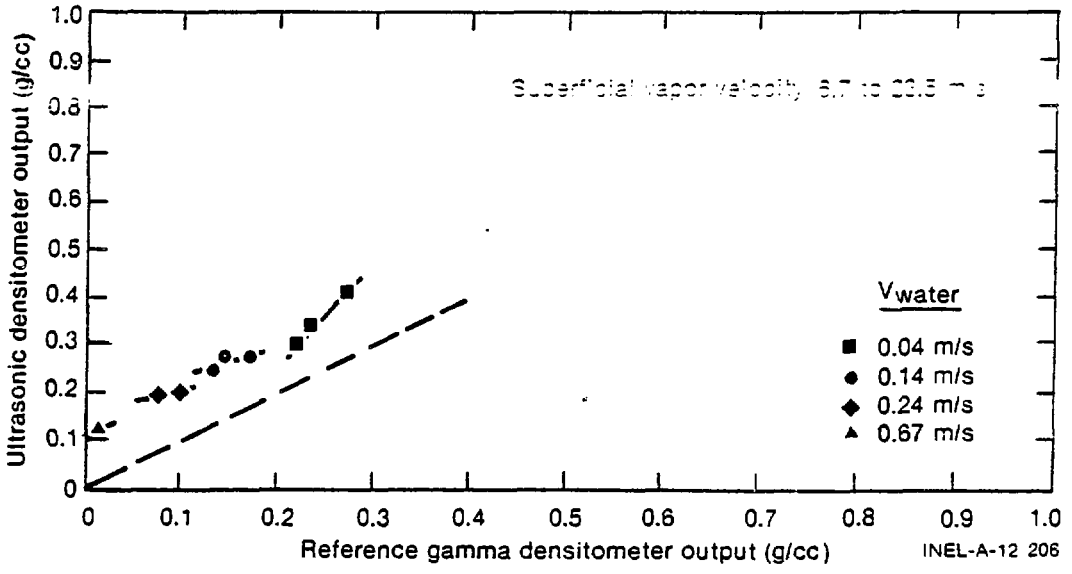

Fig. 22 Ultrasonic versus gamma densitometer mist flow data.

To increase understanding of sensor performance in different flow regimes, the test data points are plotted on a 1.72-MPa steam-water flow regime map by Mandhane[9] for horizontal flow. Dotted lines are placed on the map to separate the sensor air-water data points in terms of flow regimes as shown in Figure 25. The flow effects,

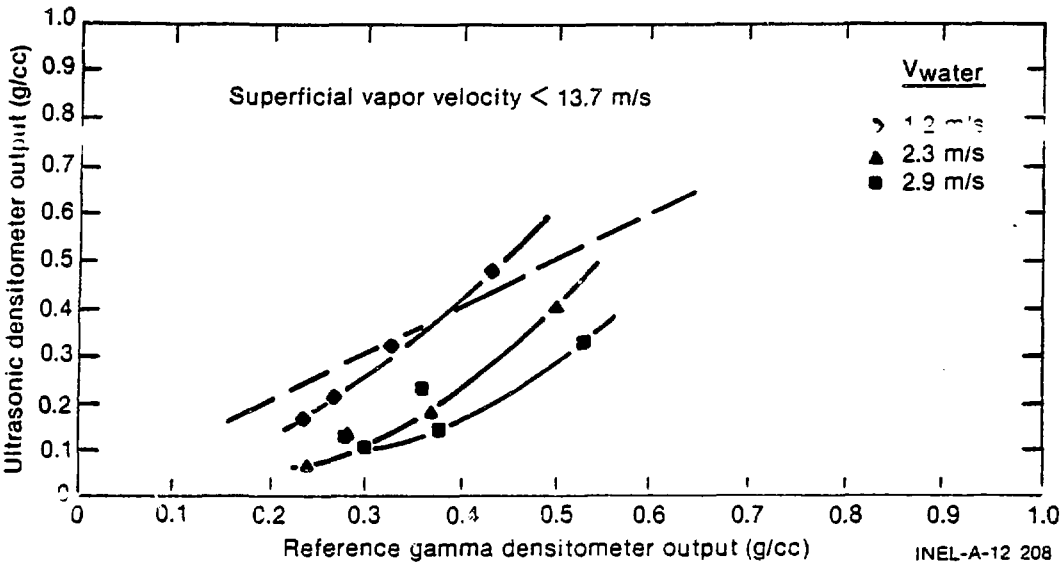

Fig. 23 Ultrasonic versus gamma densitometer slug flow data.

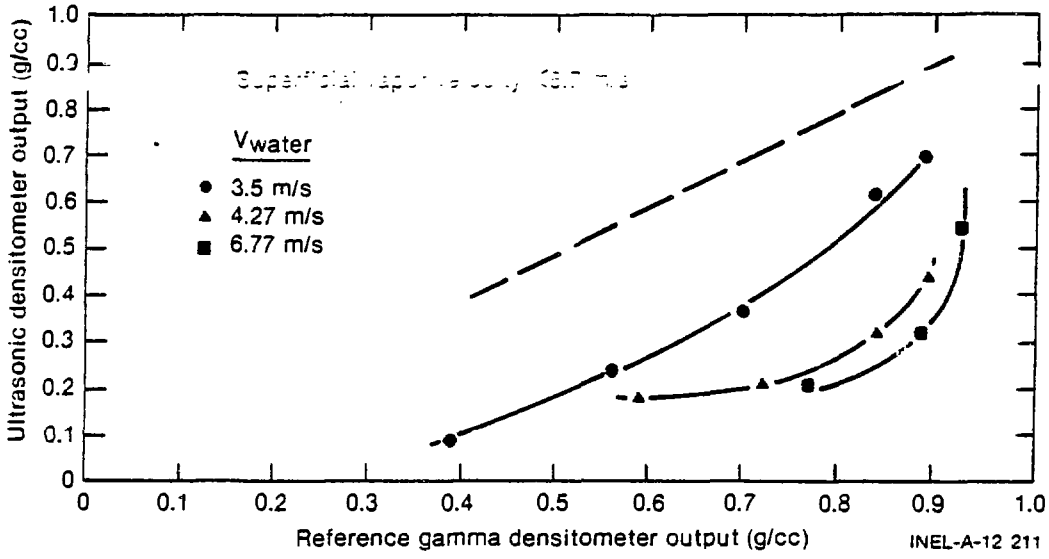

Fig. 24 Ultrasonic versus gamma densitometer dispersed bubbly flow data.

recirculation zones generated by flow separations, which compromise the detector performance, can be identified with data points that are in groups similar to the characterized steam-water flow regimes.

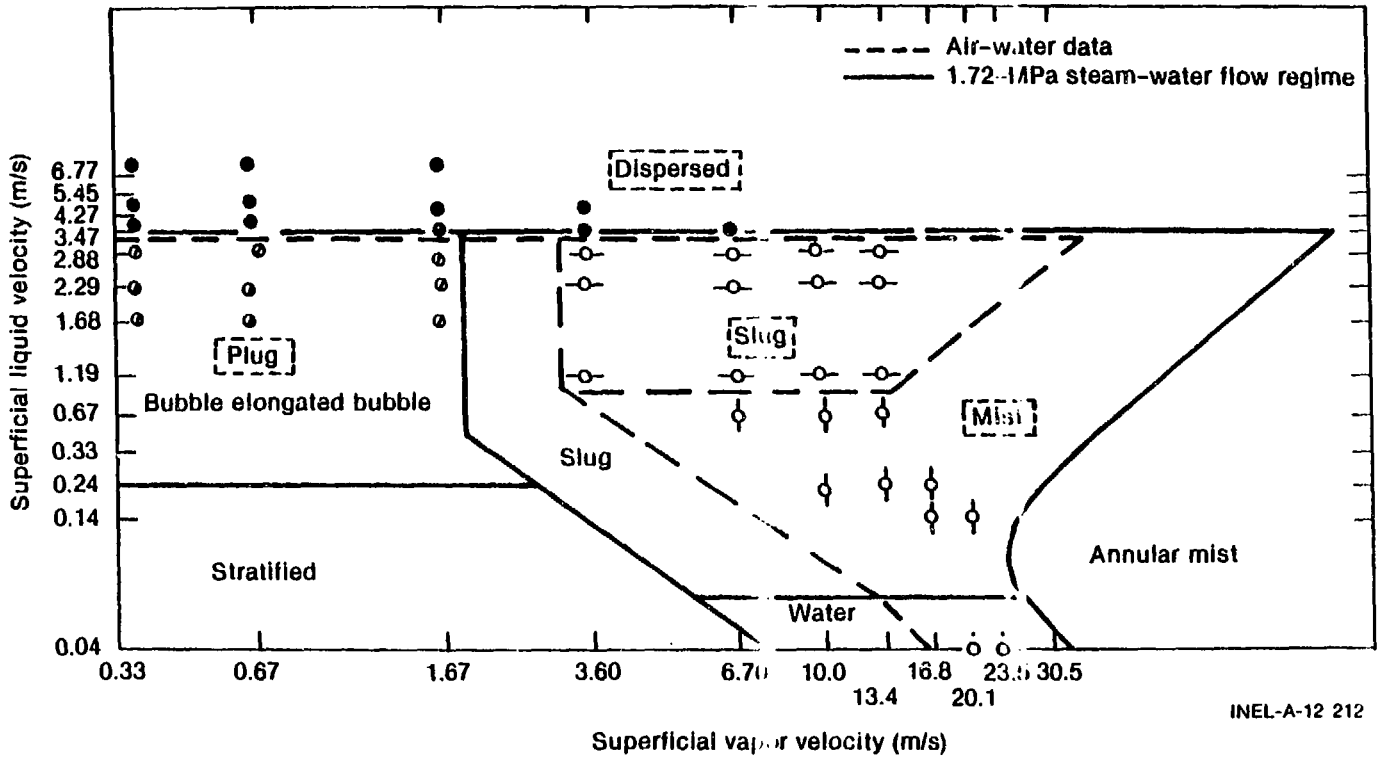

Fig. 25 Air-water test points versus flow regime.

Correlation between the gamma densitometer and the ultrasonic densitometer varied from excellent to poor depending on the flow regime. The results are analyzed best when stratified and plug, mist, slug and elongated bubble, and dispersed flows are considered separately as shown in Table III.

TABLE III

AIR-WATER FLOW DATA VERSUS FLOW REGIME

Superficial Water Velocity (m/s)	Superficial Gas Velocity (m/s)	Flow Regime	Agreement in Data
<2.3	<1.8	Stratified and plug	Excellent
<1.5	6.7 to 23.5	Mist	Good
1.0 to 2.9	3.0 to 14.0	Slug and elongated bubble	Partial
<3.0	<10.0	Dispersed and bubbly	Poor

For stratified and plug flow, the agreement was excellent as shown in Figure 21. The agreement is due to no flow separation at the lower flow rates (less than 2.9-m/s liquid and less than 1.8-m/s gas). As water flow increases beyond 2.3 m/s and is perpendicular to the front edge of the rectangular sensor, a recirculation zone builds up on the edges and is dominated by the gas bubbles. This effect masks out part of the probe sensitivity.

For mist flow, the agreement was good. In mist flow (less than 1.5-m/s water and 6.7- to 23.5-m/s gas), the probe is sensing the presence of water droplets. As the droplets strike the front edge of the probe, they are captured in the recirculation zones along the side surfaces. This capture makes the density appear to be higher than it really is. Figure 22 shows the average values of these data points.

For slug flow, the agreement was limited. In slug flow (1- to 2.9-m/s water and 3- to 14-m/s air), the velocity of the water is high enough to cause flow separation and generate a recirculation zone on the side of the probe. The amount of probe area masked by gas capture in this zone varies with superficial water velocity, void gradient, and the height of the water slugs. Average data values are plotted in Figure 23. Masking of the sensor by gas in the recirculation zone can only exist for the portion of the sensor in bubbly flow and is not stable because of the variations in the flow pattern over the length of the sensor.

For dispersed bubbly flow, the agreement was poor. In dispersed bubbly flow (greater than 3-m/s water and less than 10-m/s gas), a large stable bubble mask is formed in the recirculation zone on the surface of the sensor. This bubble mask prevents the sensor from seeing the true density. Data are plotted in Figure 24.

The transient steam-water flow test was conducted to define the performance of the LOFT core inlet 2.28- x 6.35- x 34.92-mm oval sensor shown in Figure 18 in a PWR environment by comparison of results with those from a gamma densitometer with a single beam over approximately the same vertical path. The initial conditions for the blowdown facility in which the test was performed were 5.37 MPa and 257^{o}C. The ultrasonic density detector output was corrected for temperature sensitivity and compared with the output of the gamma densitometer on the same graph shown in Figure 26. For the first 40 s of the 120-s blowdown, the agreement between the two measurements is good; but for the next 50 s, a deviation as large as 10% of range occurs. This higher density deviation from the gamma densitometer is attributed to water holdup in the recirculation zone at the surface of the sensor as experienced in the air-water mist flow data discussed above. The good agreement for the first 40 s of blowdown is attributed to the velocity of the steam-water mixture being low enough that the flow did not separate from the surface of the sensor as experienced in the air-water dispersed and bubbly flow as described previously.

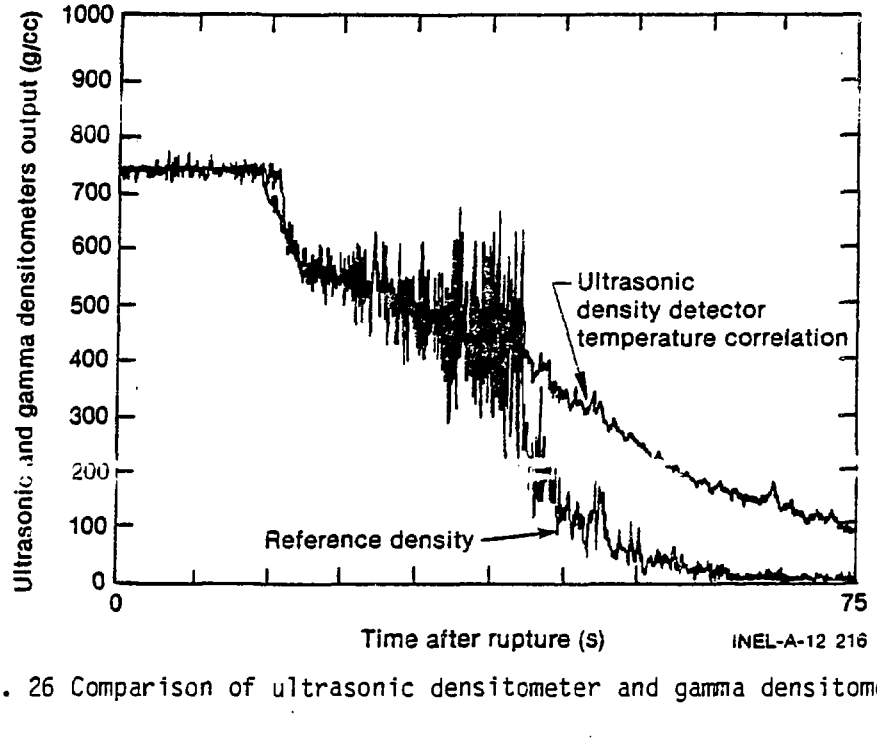

Fig. 26 Comparison of ultrasonic densitometer and gamma densitometer.

8. CONCLUSIONS

The ultrasonic densitometer sensor performs well for many flow applications. The ultrasonic densitometer and the commonly used gamma densitometer measure the same media properties but are different in that the former yields an intrusive measurement for use in the vessel and the latter yields a nonintrusive measurement for piping applications. The ultrasonic intrusive measurement does not have as high an accuracy because flow effects alter the density at the sensor surface. The air-water flow effects in a 63.5-mm inside diameter horizontal pipe are significant for 1.6- x 6.3-mm sensor bar configuration for superficial water velocities greater than 3.0 m/s. If the application is to measure the two-phase density in a pipe, the shape of the sensor should be made hydrodynamic to minimize these effects. For reactor vessel applications with vertical free-field multidirectional flow for superficial water and vapor velocity less than 3.0 m/s, the flow regime will be mostly slug and froth. For this case, the 1.6- x 6.3-mm rectangular sensor will perform well as shown

by the good correlation of the results from the ultrasonic densitometer with the results from the gamma densitometer in the air-water tests.

Survivability of the ultrasonic density detector is excellent with the all stainless steel interfaces to the corrosive PWR environment and the use of transducer materials that have $>10^{18}$-n/cm^2 radiation resistance and temperature cabability greater than 650°C.

Design of the ultrasonic sensor and transducer have configuration capabilities that will allow measurements between fuel rods in a nuclear reactor and electrically heated cores in vessel between fuel rods. Application of the design parameters described previously to a specific two-phase density and spatial measurement requirements will require construction of a prototype and performance evaluation testing since the theory is general and in many cases requires use of empirical data to evaluate the design considerations.

9. REFERENCES

1. A. E. Arave, An Ultrasonic Void Fraction Detector Using Compressional Stress Waves in a Wire Helix, IN-1441 (October 1970).

2. A. E. Arave, Ultrasonic Liquid Level Detector Using Surface Wave Attenuation in a Tube, ANCR-1047 (January 1972).

3. A. E. Arave, An Ultrasonic Liquid Level Detector Using Shear Wave Attenuation in a Bar, IN-1422 (November 1970).

4. L. C. Lynworth, "Slow Torsional Wave Sensors," Proceedings of IEEE Ultrasonic Symposium, 1977.

5. W. Shurtliff, A. Arave, and E. Fickas, "Ultrasonic Void Fraction Detector for In-Core Dynamic Measurements," Proceedings of the Twenty-Fourth International Instrumentation Symposium, 24, 1978.

6. A. E. Arave, E. Fickas, "Progress Report on LOFT Ultrasonic Density Detector for Fuel Inlet Blowdown Measurements," Proceedings of NUREG Two-Phase Flow Instrumentation Review Group Meeting, March 1978.

7. A. E. Arave, F. E. Panisko, High Temperature Ultrasonic Thermometer In-Reactor Fuel Rod Centerline Temperature Test Results, ANCR-1091 (October 1972).

8. A. E. Arave, J. Buchenauer, Use of Tungsten - 2% Thoria Ultrasonic Transmission Line and Sensor to Improve the Performance of High-Temperature Ultrasonic Thermometry, TREE-NUREG-1021 (November 1976).

9. Mandhane et al, Instrument Journal Multiphase Flow, p 537-53, (1974).

ACKNOWLEDGMENTS

Recognition is given to Larry Lynworth of Panametrics, Inc., for identification of the sensor technique, Grant Cheevers and Mike Dacus for mechanical prototype designs, Al Donaldson for materials suggestions, Dave Collins and Stan Englert for prototype fabrication, and Charles Jeffery for test engineering support.